RESEARCH ARTICLE

Incorporation of Zinc Oxide Nanoparticles in RHA-MTW Zeolite and its Application for Degradation of Dye

Babak Azari[1], Afshin Pourahmad[1,*], Babak Sadeghi[2], Masoud Mokhtary[1]

[1] Department of Chemistry, Faculty of Science, Rasht Branch, Islamic Azad University, Rasht, Iran.

[2] Department of Chemistry, Faculty of Science, Tonekabon Branch, Islamic Azad University, Tonekabon, Iran.

ARTICLE INFO

Article History:
Received 2020-02-04
Accepted 2020-03-05
Published 2020-08-01

Keywords:
Environmental Catalysis
Green Chemistry
Photocatalysis
Nanoporous Materials
Nanocomposites

ABSTRACT

White rice husk ash (RHA), an agricultural waste, was used as a silica source for MTW zeolite synthesis. The RHA-MTW zeolite derived from RHA was prepared by hydrothermal method at 150 °C in the presence of tetraethylammonium hydroxide. ZnO nanoparticles (NPs) were grown in zeolite substrates using a solid state reaction. The synthesized nanocomposite (NC) was characterized by XRD, SEM, DRS and TEM and tested as photocatalytic degradation of methylene blue (MB) dye from aqueous solution under ultraviolet (UV) light. The BET results indicated that pore volume and surface area of ZnO/RHA-MTW NC was smaller than RHA-MTW zeolite. On the basis of the obtained experimental results, it was found that zinc oxide NPs were encapsulated into the channels of RHA-MTW zeolite. The SEM and TEM images of ZnO/RHA-MTW NC confirmed the formation of RHA-MTW particles with size diameter of 2.5 µm and locating of zinc oxide NPs in channels of zeolite with an average size of between 35 nm. The results showed MB degradation had reached 85 % under UV light. The MB indicated maximum adsorption at pH=9. The photocatalytic activity of ZnO was enhanced in the presence of zeolite due to reduction of recombination rate of the electro-hole in ZnO semiconductor.

How to cite this article
Azari B., Pourahmad A., Sadeghi B., MokhtaryM. Incorporation of Zinc Oxide Nanoparticles in RHA-MTW Zeolite and its Application for Degradation of Dye. J. Nanoanalysis., 2020; 7(3): 179-189. DOI: 10.22034/jna.002.

INTRODUCTION

The pollution increment in the environment is assuredly one of the major hazards to human health. Selective and sensitive detection of hazardous materials as well as an effective procedure for their treatment are important steps for decreasing the effects of environmental pollutants [1]. The removal of hazardous materials from underground water and ground is biotic for human being. Over the past two decades, the photocatalytic degradation of these materials on the surface of semiconductors has become an important area of catalytic research [2, 3]. Rice husk is combined of both organic (about 75–80%) and inorganic components (about 20–25%). After removing organic content, the ash contained SiO_2 with a purity of about 90% [4]. The purity of rice husk silica (RHS) could be modified by taking out inorganic components in the husk such as oxides of Ca or Al with mineral acid before burn [5]. The RHS could be utilized as a SiO_2 source for preparation of a number of porous materials such as zeolite ZSM-5, zeolite LSX, and MCM-41. MTW is a silica rich zeolite with unidimensional 12-membered ring channel system and pore openings of 5.7 × 6.1 Å [6], which are slightly larger than that of MFI type zeolite. MTW is an attractive catalyst for applications such as isomerization and alkylation of aromatic hydrocarbons and so its appropriate matrix for the preparation of highly dispersed semiconductor NPs. On the other hand, zinc oxide is an important semiconductor as a photocatalyst. It is a large band gap (3.37 eV) semiconductor having the advantages of ease of synthesis, non-toxicity and low cost [7, 8]. Last

* Corresponding Author Email: *pourahmad@iaurasht.ac.ir*
afshinpourahmad@yahoo.com

researches showed that doping a semiconductor onto a suitable matrix has several benefits in various reactions. 1) Increases the activity of the semiconductor 2) prevent uncontrollable growth of particles 3) prevent particle aggregation 4) controls particle size [9]. In the present study, rice husk was combusted at 550 ˚C for the production of amorphous silica. The resulted amorphous RHA was then utilized as a starting material for the synthesis of MTW zeolite. The zeolite provides great opportunities as a template of nanostructured materials. Here we describe the template synthesis of ZnO NPs in RHA-MTW zeolite by solid state reaction. The new nanocomposite was used for the photodegradation of MB dye under UV light and the effects of some key operating experimental parameters were studied.

MATERIALS AND METHODS

Materials

The rice husk was collected at a local rice milling plant in the State of Guilan, Iran. Other materials used were tetraethylammonium hydroxide (40% TEAOH solution in water, supplied by Fluka Chimika), sodium aluminate (54 wt% Al_2O_3: 41 wt% Na_2O, technical grade), sodium hydroxide (Merck), Zn $(CH_3COO)_2$ (Merck), nitric acid (Merck) and distilled water. The methylene blue dye (C.I. name: Basic Blue 9, $C_{16}H_{18}ClN_3S{:}3H_2O$) was purchased from Fluka company.

Preparation of rice husk ash

To prepare RHA, about 7.5 g of clean rice husk (RH) was stirred with 187 mL of 1.0 mol L^{-1} nitric acid at room temperature for 24 h. Acid treated RH was washed with a large amount of distilled water to constant pH, dried in an oven at 100 ˚C for 14 h and burnt in a muffle furnace at 550 °C for 6 h to obtain white RHA.

Preparation of RHA-MTW from RHA

The reaction mixture was prepared at room temperature with the appropriate amounts of reagents needed to obtain a total weight of 17 g as follows. A 3.7 g portion of RHA was added to the solution of 0.12 g NaOH in 9 g of water in a Teflon beaker to give mixture A. Sodium aluminate (0.4 g) was dissolved in the TEAOH solution (7.9 g), which was previously diluted with a small amount of water (1.5 g), to yield solution B. Solution B was added slowly to mixture A with vigorous stirring and homogenized for at least 3 h. The chemical composition of the initial gel was $1.96Na_2O$: $27SiO_2$: Al_2O_3: $5TEA_2O$: $240H_2O$. The gel obtained was transferred to a stainless steel autoclave and heated at 150 ˚C under autogeneous pressure for 6 days. After hydrothermal crystallization, a solid?? was separated from the mother liquor by filtering and was washed with distilled water until neutral. Finally, the solid was dried at 110 ˚C overnight. After filtration, washing and drying, the solids were calcined at 550 ˚C for 8 h. The resultant solid was cooled to the ambient temperature and weighed.

Synthesis of ZnO nanoparticles in prepared RHA-MTW

The ZnO/RHA-MTW NC were prepared by solid state reaction of 0.5 g of zeolite with 0.18 g of $Zn(CH_3COO)_2$. After mixing, the solid phase samples were calcined in airflow at 550 °C for 6 h.

Characterization

Powder X-ray diffraction patterns of the samples were recorded using an X-ray diffractometer (Bruker D8 Advance) with Co–Kα radiation (λ = 1.789 Å) under the conditions of 40 kV and 30 mA, at a step size of 2θ = 0.02°. The transmission electron micrographs (TEM) were recorded with a Philips CM10 microscope, working at a 100 kV accelerating voltage. Samples for TEM were prepared by dispersing the powdered sample in acetone by sonication and then drip drying on a copper grid coated with carbon film. The surface morphology of the samples was obtained using a JeolJSM-5610 LV scanning electron microscopy (SEM). All samples were analyzed in random orientation. The UV–vis diffused reflectance spectra (UV–vis DRS) were obtained with a UV–vis Scinco 4100 spectrometer with an integrating sphere reflectance accessory. $BaSO_4$ was used as reference material. The specific surface area and pore diameter were measured using Brunauer-Emmett-Teller (BET) Analyzer, Model BEL SORP mini II.

Photocatalytic activity

Photocatalytic device consists of a cylindrical glass tube and the built-in light source surrounding a quartz sleeve. The ultraviolet light was carried out by using a 125 W Hg-lamp with maximum emission at approximately 313.2 nm. The photoreactor was filled with 100 mL of 3–20 ppm of dye as pollutant and 0.03–0.1 g/L of photocatalyst. The whole reactor was cooled with water-cooled jacket on its outside

and the temperature was kept at 25 ˚C. All reactants in the reactions were stirred using a magnetic stirrer to ensure that the suspension of the catalyst was uniform during the course of the reaction. To determine the percent of the destruction of the dye, the samples were collected at regular intervals, and centrifuged to remove the nanocatalyst particles that exist as undissolved particles in the samples. Some experiment was performed to observe MB decolorization and degradation in the absence of nanocomposite (photolysis). The photocatalytic activity was evaluated in terms of decolorization (oxidation of chromophore group) and degradation (oxidation of aromatic group) efficiencies. The decolorization and degradation efficiencies were calculated with respect to the change in intensities of absorption peaks at 664 nm (λ_{max} of MB) and 280 nm (representative λ for aromatic carbon content) by using the equation:

$$\%D = 100 \times [A_o - A_t/A_o]$$

Where A_o is the equilibrium absorbance at 664 and 285 nm after adsorption–desorption equilibrium and A_t is the absorbance at 664 and 285 nm after a certain irradiation time (min). The absorption of the solution was measured by a UV–vis spectrophotometer shimadzu model 1600 PC. In order to obtain maximum degradation efficiency, pH, concentration of the dye and the amount of photocatalysts were studied in amplitudes of 3–11, 3–20 ppm and 0.03–0.1 g/L, respectively.

RESULTS AND DISCUSSION

Structure analysis of samples

The powder XRD pattern of the RHA, RHA-MTW, and ZnO/RHA-MTW samples are presented in Fig. 1. A very broad peak in the range of 18–23° (2θ) was observed as a result of the amorphous nature of the SiO_2 [10]. The XRD profile of RHA-MTW zeolite was matched quite well with a pattern that was given in the literature [6] which allowed up identifying the product as MTW zeolite. The XRD patterns of ZnO/RHA-MTW NC not only show peaks related to zeolite, but also indicate additional peaks at 2θ= 31.8, 34.5, 36.3, 47.5, 56.5, 62.9, 66.3, 68.1, and 69.3 ° corresponding to (100), (002), (101), (102), (110), (103), (200), (112), and (201) planes respectively which are assigned to zinc oxide NPs (JCPDS No. 80-0074) [11].

Electron microscopy study

Fig. 2 shows SEM micrographs of SiO_2 derived from a rice husk, RHA-MTW, and ZnO/RHA-MTW NC. SEM image of SiO_2 indicated the outer epidermis of synthesized SiO_2, which is well organized and has a corrugated structure. The SEM image of synthesized SiO_2 was similar to rice husk [10] because during calcination, only organic compounds in rice husk were removed. The morphologies of the RHA-MTW and ZnO/RHA-MTW samples showed greater similarity to each other, taking the form of large rounded aggregates (uniform size with a diameter about 2.5 μm). This size was similar to that of the commercial MTW, which was synthesized by the same method [12.]. RHA-MTW was composed of single-crystal nanoparticles with diameters of 25-30 nm that increased in size (30-40 nm) with incorporating zinc oxide in zeolite.

The RHA-MTW and ZnO/RHA-MTW samples were characterized by TEM. The TEM results (Fig. 3) showed that the samples possessed a highly heterogeneous morphology, with particle aggregates with sizes on the order of 2.5 μm, at the outrances of which could be seen the formation of elongated structures in the form of needles, corroborating the SEM results [13]. TEM images of ZnO/RHA-MTW demonstrated that zinc oxide nanoparticles with average diameter size 35 nm, were located into pore of zeolite.

BET and BJH results

N_2-adsorption tests showed typical type-I adsorption–desorption curves, thus indicating that the RHA-MTW and ZnO/RHA-MTW sample had a remarkable microporous structure according to the IUPAC classification (Fig. 4) [14]. DFT calculations showed that the RHA-MTW and ZnO/RHA-MTW samples possessed one peak at 1.29 and 1.37 nm, which correspond to micropores, respectively. The volume of micropores in RHA-MTW and ZnO/RHA-MTW were 0.11 and 0.03 $cm^3\ g^{-1}$, respectively. The BET surface area was 330 and 210 $m^2\ g^{-1}$ for RHA-MTW zeolite and ZnO/RHA-MTW NC, respectively. The decrement of ZnO/RHA-MTW NC pore volume and surface area with respect to RHA-MTW zeolite declared that zinc oxide NPs were encapsulated into the channels of RHA-MTW zeolite. This result was in agreement with ZnO/RHA-MTW TEM image.

Study of UV–vis diffuse reflectance spectra

The UV–vis diffuse reflectance spectra were measured to examine the light absorption properties

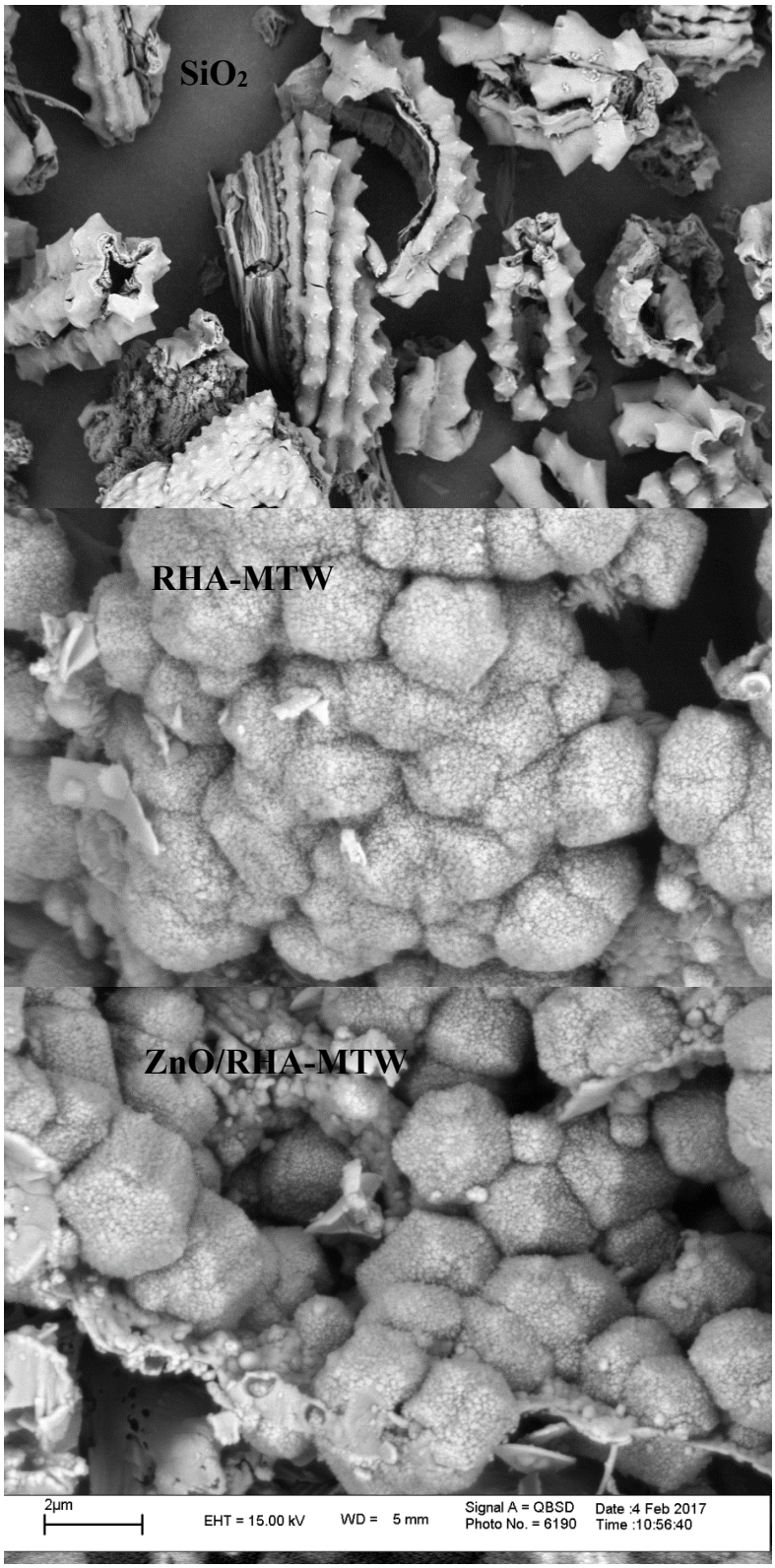

Fig. 2. SEM images of samples.

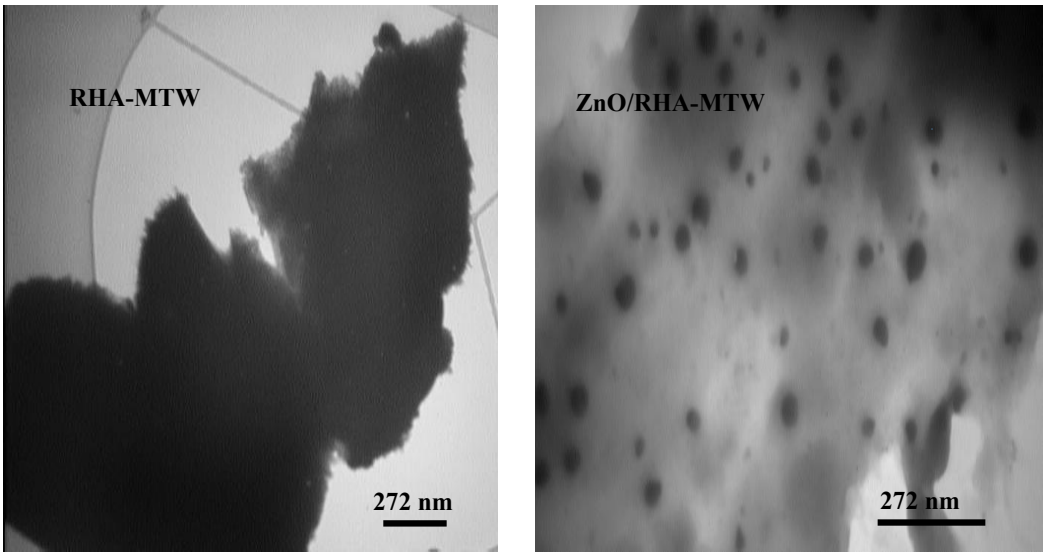

Fig. 3. TEM images of samples.

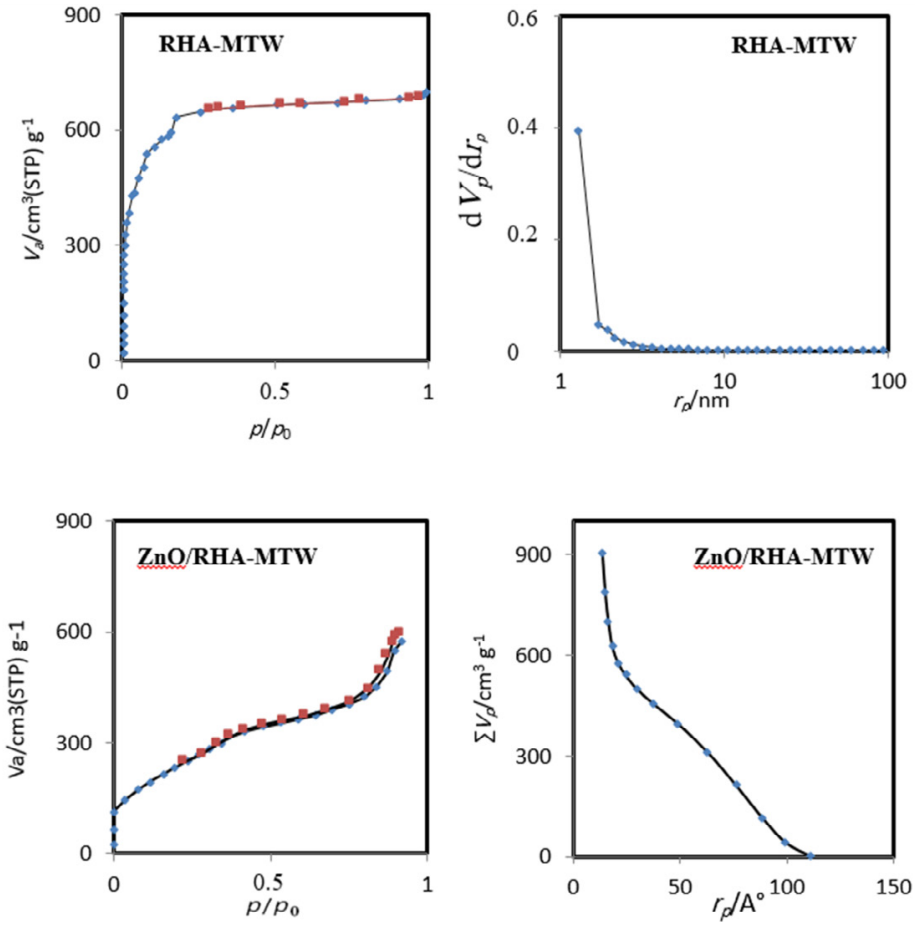

Fig. 4. N_2 adsorption–desorption isotherms and BJH pore size distribution of the RHA-MTW and ZnO/RHA-MTW samples.

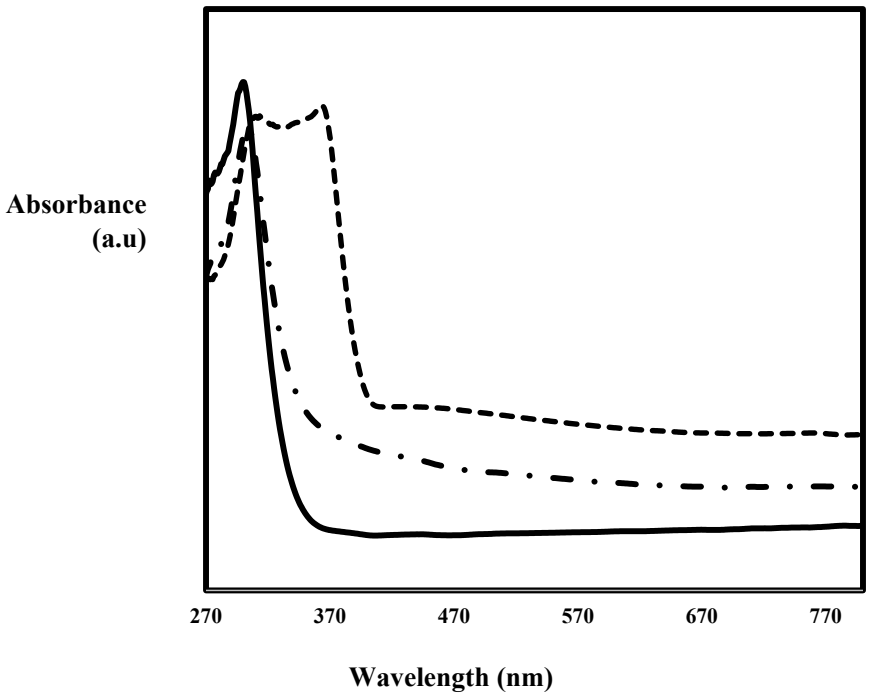

Fig. 5. Diffuse reflectance spectra of samples.

of the prepared samples and are displayed in Fig. 5. Each sample showed dramatically different UV–vis absorption characteristics. The color of the zinc oxide NPs, RHA-MTW, and ZnO/RHA-MTW NC was white. The diffuse reflectance spectrum of RHA-MTW showed a peak at 295 nm could be related to the charge transfer band for aluminum atoms in extra-framework and the framework of RHA-MTW zeolite, which was similar to the literatures [15].

The absorption edges (or the band gap) was determined from plots of $[\alpha h\nu]^{1/2}$ versus $h\nu$. The ZnO NPs showed an absorption edge at ~ 400 nm (band gap energy ~3.1 eV), which band gap energy was less than pure ZnO (~ 3.37 eV) [16]. Band gaps energy of 3.48 (ca. 356 nm) and 2.58 eV (ca. 480 nm) were observed for ZnO in the ZnO/RHA-MTW NC and RHA-MTW zeolite, respectively. The estimated optical band gap energy value of ZnO in ZnO/RHA-MTW NC was higher than that of ZnO NPs (3.1 eV), which was attributed to the quantum confinement effect arising from the small crystal size. So, due to band gap energy bigger than 3 eV the synthesized nanocomposite could sufficiently absorb UV light and possess favorable photocatalytic properties under UV-light irradiation.

Photocatalytic activity of nanocomposite

The photocatalytic activity of ZnO/RHA-MTW photocatalyst was evaluated by photocatalytic decomposition of methylene blue (Fig. 6). Prior to irradiation, the MB solution over the photocatalyst was kept in the dark for 30 min to obtain the equilibrium adsorption state. After 30 min of irradiation under UV light in a ZnO/RHA-MTW photocatalyst suspension, 90.00% of dye (15 ppm) was decomposed and degradation of the solution was observed at pH 6.5. Besides, no new bands appear in the UV–Vis region due to the reaction intermediates formed during the degradation process. The photocatalytic performance of the resultant photocatalysts was evaluated in λ = 664 nm by photodegradation of MB as a contaminant under visible light irradiation. In the absence of photocatalyst and pure RHA-MTW, MB self-degradation was almost negligible. Table. 1 shows the MB degradation over ZnO, RHA-MTW zeolite and the ZnO/RHA-MTW photocatalysts. RHA-MTW sample no showed significant degradation for MB dye after 30 min but was adsorbed ~50% dye over its surface due to high surface area. But ZnO NPs and ZnO/RHA-MTW NC due to separation process of the photogenerated electrons and holes accelerates in the ZnO semiconductor

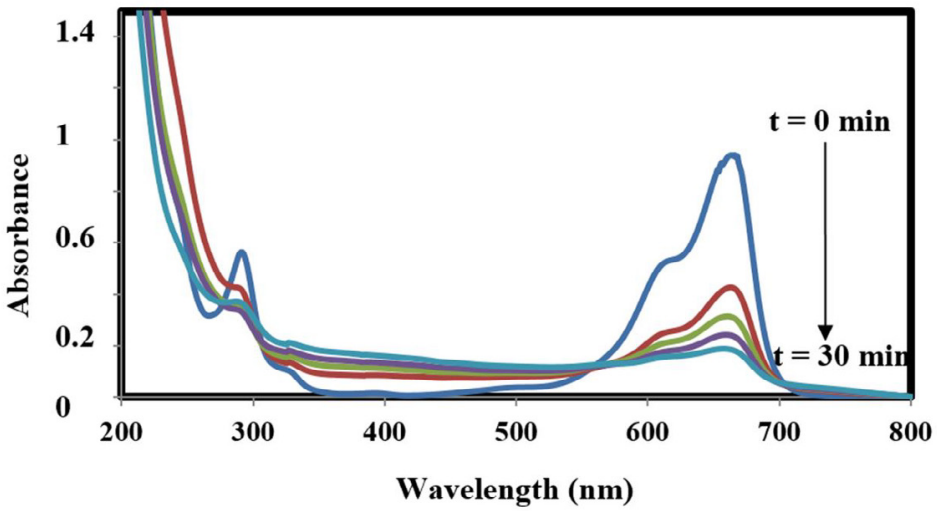

Fig. 6. Spectra change that occur during the photocatalytic degradation of aqueous solution of methylene blue: pH = 6.5, ZnO/RHA-MTW photocatalyst = 0.08 g/L, C_o = 15 ppm after 30 min.

Table 1. The degradation percent of MB aqueous solution over different samples under UV light, C_o = 15 ppm, the amount of photocatalysts 0.08 g/L, pH=6.5, degradation time = 30 min.

photocatalysts	% degradation of MB dye	%decolorization of MB dye
ZnO NPs	30.00	35.00
ZnO/RHA-MTW	85.00	90.00
RHA-MTW	5.00	6.00
light	-	4.00

under UV light and photodegradation of MB was increased [17]. Photodegradation of ZnO/RHA-MTW NC was more than ZnO NPs. This result indicated that the introduction of RHA-MTW zeolite plays an active part in the adsorption and catalytic degradation process of MB dye. Two reasons may account for the enhanced catalytic activity of them: (1) RHA-MTW zeolite can adsorb more MB dye molecules on its surface. (2) Due to existence aluminum atoms in its structure, RHA-MTW zeolite can act as an electron acceptor allowing for the photo-excited electrons of ZnO in the composites to be quickly transferred from the conduction band of ZnO to RHA-MTW zeolite.

EFFECT OF EXPERIMENTAL PARAMETERS

Effect of nanocomposite amount

In order to determine the optimal amount of photocatalyst, some experiments were performed at pH 6.5 by varying the amount of photocatalyst from 0.03 to 0.1 g/L. The optimum NC amount of degradation of methylene blue dye was 0.08 g/L. It was observed that the degradation rate enhanced by increase in photocatalysts amount from 0.03 to 0.08 g/L. This was probably due to increase in the number of photocatalysts that increased the number of photons and dye molecules absorbed. Increase of the photocatalysts amount to more than 0.08 g/L, degradation rate decreased. This phenomenon may be explained by the opacity and light scattering of photocatalyst at high concentration, load to decrease in the passage of irradiation through the sample [18, 19].

Effect of concentration of dye

For determination of the optimal amount of dye, photocatalytic degradation was checked out with various concentrations of dye from 3-20 ppm at pH 6.5 with 0.08 g/L NC. The degradation efficiency of dye was decreased by increasing the initial concentration of dye to more than 15 ppm. The decrease of degradation efficiency to increase of concentration of dye can be due to two reasons. By increasing the amount of dye, more dye molecules

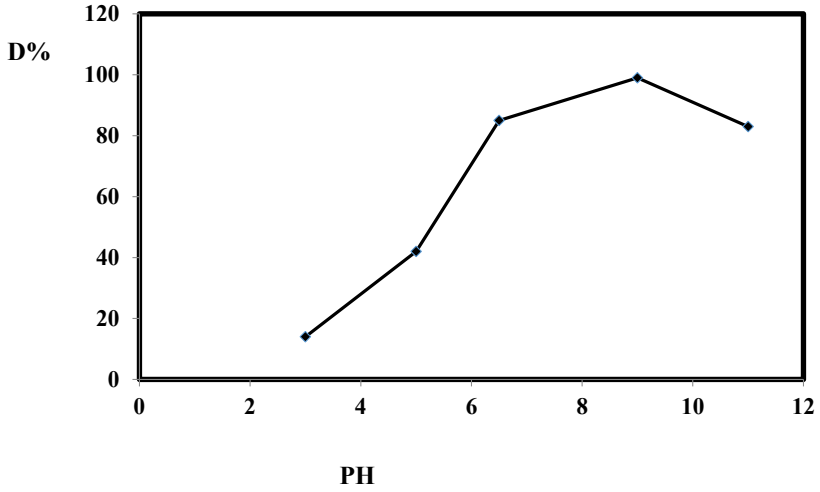

Fig. 7. Change in decomposition % aqueous solution of methylene blue as a function of pH: ZnO/RHA-MTW photocatalyst = 0.08 g/L, C_o = 15 ppm.

will be adsorbed on the surface of the photocatalyst and the active sites of the photocatalysts will be reduced. Therefore, with increase occupied spaces of photocatalyst surface, the generation of hydroxyl radicals will be decreased. Increasing concentration of dye can also be lead to decrease in the number of photons that will be arriving to the surface of NC. The more light is absorbed by molecules of dye and the excitation of photocatalyst particles by photons will be reduced. Thus, photodegradation efficiency diminished [19].

Effect of pH

The pH of the solution affects the photodegradation processes due to the strongly pH dependent of the properties such as semiconductor's surface charge state, flat band potential, and dissociation of compounds in the solution. Photodegradation of dye (15 ppm) was studied in amplitude pH of 3–11 in the presence of nanocatalysts (0.08 g/L). The results from the irradiation time of 30 min showed that (Fig. 7), in the presence of photocrystal and at pH 9.0, 99.00% degradation efficiency was obtained. The pH of point of zero charge (pH_{pzc}) calculated for the ZnO nanoparticles and RHA-MTW are 8.8 and 5.5 respectively [20]. The pH_{pzc} related to ZnO/RHA-MTW played an important role in the degradation of MB dye. Because the dye first was adsorbed on the surface RHA-MTW zeolite, then decomposed by $^{\bullet}OH$. The charge of the photocatalyst surface was positive and negative at pH values smaller and higher than the core-shell pH_{pzc}, respectively. Hence, at pH values smaller than pH_{pzc}, the repulsion between the positively charged surface of the ZnO/RHA-MTW photocatalyst and positive groups of MB molecules decreases the photodegradation efficiency. At pH values higher than pH_{pzc}, the surface of the catalyst was slightly negatively charged, and the coordinative interaction with positive $R_2 = N^+ = R^/$ group of MB was increased. Meanwhile, demethylation and photo degradation of methylene blue are observed in the presence of the ZnO/RHA-MTW photocatalyst at pH_s above 11 [21].

Formation of reactive species

During the photocatalytic oxidation process, a large number of reactive species including $\bullet OH$, h^+, H_2O_2, and $^{\bullet}O_2^-$are produced. To investigate the underlying mechanism of degradation of the MB dye, various scavengers of reactive species were added to the reaction system and their effect on the photodegradation efficiency was examined. Isopropyl alcohol (IPA) was added to the system to quench $^{\bullet}OH$ [22] whereas benzoquinone (BQ) [23], Catalase (CAT) [23] and ethylene diamine tetraacetic acid (EDTA) [24] were added as $^{\bullet}O_2^-$, H_2O_2, and h^+ scavengers respectively. The results are shown in Table 2. As clear from the Table 2, catalase exhibit weaker effect on the photocatalytic degradation efficiency of ZnO/RHA-MTW NC indicating that H_2O_2 are not primary reactive species in the photocatalytic oxidation process and

Table 2. The photogenerated active species trapped in the system of photodegradation of MB by ZnO/RHA-MTW photocatalyst under UV light irradiation.

samples	IPA(•OH)	BQ (•O_2^-)	CAT (H_2O_2)	EDTA (h^+)	No scavenger
%D ZnO/RHA-MTW	14.0	18.0	83.0	20.0	85.0

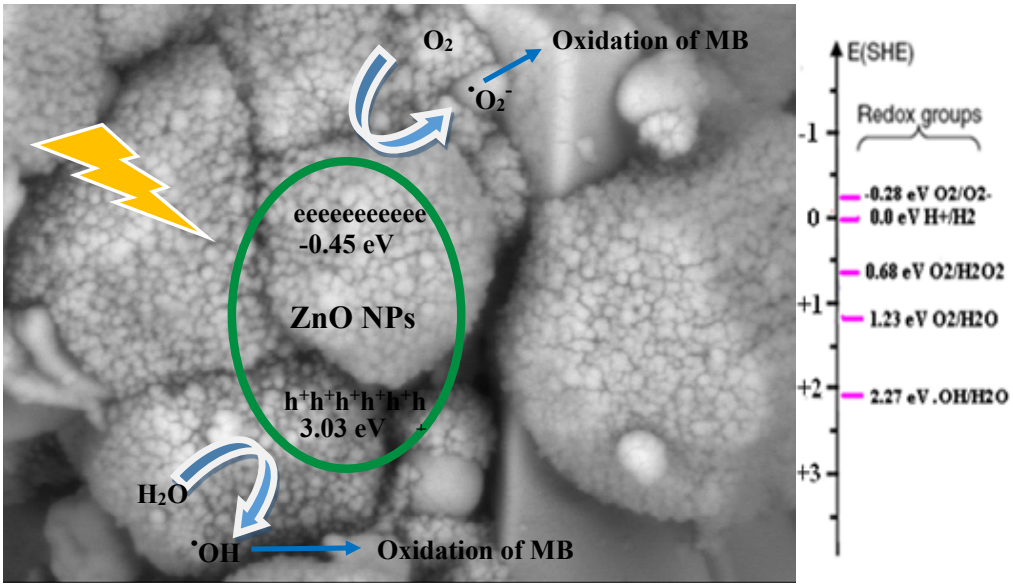

Fig. 8. Schematic illustration for the proposed mechanism of photocatalytic degradation of MB by ZnO/RHA-MTW photocatalyst.

thus played a minor role. The addition of IPA, BQ and EDTA had a significant effect on degradation efficiency of ZnO/RHA-MTW photocatalyst compared with no scavenger under the same conditions indicating the main role of •OH, •O_2^- and h^+ as reactive species in photocatalytic oxidation process. With the addition of IPA, EDTA or BQ, the degradation value decreases significantly, indicating that •OH, h^+ and •O_2^- are primary reactive species.

Photocatalytic reaction mechanism

To ascertain the capability of each particular composite material to photodegradation organic chemicals in the visible range of the spectrum, one needs to analysis the UV–Vis diffuse reflectance spectra. The results in 3.4 section indicated that the flower–shaped ZnO NPs was a UV driven light photocatalyst with band gap higher than 3.1 [25]. Fig. 6 showed that ZnO/RHA-MTW photocatalyst can be used as efficient photocatalysts under UV light irradiation. The conduction and valence band positions in the semiconductor at the point of zero charge can be calculated by the following formula [26, 11]:

$$E_{V_R} = X - E_e + 0.5E_g$$

Where E_{V_R} is the potential of the valence band, X is the electronegativity of the semiconductor which was the geometric mean of the electronegativity of the constituent atoms. The electronegativity value for ZnO was 5.79 eV [16]. The E_e was the energy of free electrons on the hydrogen scale (4.5 eV) and E_g was the band gap energy of the ZnO semiconductor in RHA-MTW zeolite. In the present study, the band gap energy of the ZnO semiconductor in RHA-MTW zeolite was 3.48 eV. The E_{V_R} and E_{C_R} were calculated 3.03 and -0.45, respectively. As shown in Fig. 8, in ZnO/RHA-MTW photocatalyst, ZnO NPs (Eq. 1) can absorb UV light to produce plasmon-induced electrons and holes. The conduction band (C_B) and valence band (V_B) energy levels of ZnO were calculated ca. -0.45 and 3.03 eV *vs.* SHE, respectively. From the photochemistry point of view, it was possible to reduce O_2 to •O_2^-, E° (O_2/•O_2^-= −0.28 V/SHE) [28] through one electron reduction process because

the C_B potential of ZnO (-0.45 eV *vs* SHE) was more negative than the single electron reduction potential of oxygen (Eq. 2). The photogenerated holes from the valence band of ZnO (+2.99 eV) or Ag NPs will be produced of •OH of H_2O by oxidizing holes and produced radicals can be effected for the degradation of organic pollutants (Eq. 2-5). The possible, taking place photoreaction equations were listed following:

$$\text{ZnO/RHA-MTW NPs} + h\nu\ (\text{UV light}) \rightarrow \text{ZnO NPs } (h^+ + e^-)/\text{RHA-MTW} \quad (1)$$

$$O_2 + \text{ZnO })e^-_{CB}) \rightarrow {}^{\bullet}O_2^- + \text{ZnO} \quad (E^0 = -0.28\ \text{V, vs. SHE}) \quad (2)$$

$$H_2O + h^+ (\text{ZnO}) \rightarrow {}^{\bullet}OH + H^+ \quad (E^0 = 2.72\ \text{V, vs. SHE}) \quad (3)$$

$$\text{Dyes} + {}^{\bullet}O_2^- \rightarrow OX_{\text{Prod}}. \quad (4)$$

$$\text{Dyes} + {}^{\bullet}OH \rightarrow OX_{\text{Prod.}} \quad (5)$$

On the other hand, RHA-MTW is a type of Zeolite with numerous active sites for the adsorption of dye molecules. It also can prevent of aggregation of NPs. Furthermore, the zeolite can be used to surmount the turbidity of the solution due to dispersion of photocatalyst. Meanwhile, separation of photocatalyst will be easy. RHA-MTW zeolite can act as acceptors due to the presence of aluminium atoms in its structure [29]. The electron from the conduction band (C_B) of ZnO in RHA-MTW zeolite can be transferred to the electron acceptor such as aluminium atoms in RHA-MTW zeolite. The electrons from these aluminium sites were then transferred to the O_2 molecules in the solution, which results in a delay in the recombination reaction.

Recycling studies

The stability of the ZnO/RHA-MTW NC was evaluated in terms of performing the MB photodegradation repeated four times. The results showed that, after four recycles for the photodegradation of MB, the catalyst does not exhibit any significant loss of activity, indicating the catalysts have good stability for photocatalysis. Therefore, we further collected the reused photocatalyst after photoreaction to check the photostability of ZnO/RHA-MTW. The diffuse reflectance spectra and XRD pattern of the ZnO/RHA-MTW does not show significant variation after recycle experiments. These results confirm that the ZnO/RHA-MTW NC was stable under our experimental conditions.

CONCLUSION

In summary, the RHA-MTW zeolite derived from RHA was prepared by hydrothermal method at 150 °C in the presence of tetraethylammonium hydroxide. ZnO (NPs) were incorporated in RHA-MTW zeolite using a solid state reaction. The formation of ZnO nanoparticles in zeolite was observed by TEM, SEM, XRD, BET and DRS. The synthesized zeolite was used in degradation of MB dye under UV-light. RHA-MTW zeolite had an important role in the increase of MB dye absorption over photocatalyst and separation of electron-hole of ZnO NPs. The results showed that ZnO/RHA-MTW photocatalyst increased the percentage of degradation methylene blue (MB) to 85.00 %. The average size of ZnO NPs over RHA-MTW was less than 35 nm. The degradation of MB in the presence of scavengers demonstrated that •OH, ${}^{\bullet}O_2^-$ and h^+ as reactive species play the main role in the photocatalytic oxidation process.

ACKNOWLEDGEMENT

The authors are grateful to the Islamic Azad University, Rasht Branch.

CONFLICT OF INTEREST

The authors declare that there is no conflict of interests regarding the publication of this manuscript.

REFERENCES

1. Liu Y., Su G., Zhang B., Jiang G., Yan B. Nanoparticle-based strategies for detection and remediation of environmental pollutants. Analyst. 2011;136:872-877.
2. Velasco L.F., Fonseca I.M., Parra J.B., Lima J.C. Ania C.O. Photochemical behaviour of activated carbons under UV irradiation. Carbon. 2012;50:249-258.
3. Pourahmad A., Deljoopour M. Design of ZnCdS quantum dots loaded on mesoporous silica as a UV-light-sensitive photocatalyst. Synth. React. Inorg. Met.-Org. Chem. 2016;46:694-700.
4. Ziksari M., Pourahmad A. Green synthesis of CuO/RHA-MCM-41 nanocomposite by solid state reaction: Characterization and antibacterial activity. Indian J Chem Sect A. 2016;55A:1347-1351.
5. Loiha S., Prayoonpokarach S., Songsiriritthigun P., Wittayakun J. Synthesis of zeolite beta with pretreated rice husk silica and its transformation to ZSM-12. Mater Chem Phys. 2009;115:637-640.
6. Dimitrov L., Mihaylov M., Hadjiivanov K., Mavrodinova V. Catalytic properties and acidity of ZSM-12 zeolite with different textures. Microporous Mesoporous Mater. 2011;143:291–301.
7. Yu J., Yu X. Hydrothermal synthesis and photocatalytic

activity of zinc oxide hollow spheres. Environ Sci Technol. 2008;42:4902-4907.
8. Luo Q-P., Yu X-Y., Lei B-X., Chen H-Y., Kuang D-B., Su C-Y. Reduced graphene oxide-hierarchical ZnO hollow sphere composites with enhanced photocurrent and photocatalytic activity. J Phys Chem C. 2012;116:8111-8117.
9. Sohrabnezhad Sh., Karkoudi N., Asadollahi A. Core–shell composite of mordenite zeolite@MCM-41mesoporous: Synthesis, characterization and application in photocatalytic activity. Colloids Surf A. 2017;520:17-25.
10. Liou T.H. Preparation and characterization of nano-structured silica from rice husk. Mater Sci Eng A. 2004;364:313-323.
11. Sohrabnezhad Sh., Seifi A. The green synthesis of Ag/ZnO in montmorillonite with enhanced photocatalytic activity. Appl Surf Sci. 2016; 386:33-40.
12. Liu Y., Guo W., Zhao X.S., Lian J., Dou J., Kooli F. Zeolite beta catalysts for n-C7 hydroisomerization. J Porous Mater. 2006;13:359-364.
13. Chaves T.F., Carvalho K.T.G., Urquieta-González E.A., Cardoso D. One-step synthesis of functionalized ZSM-12 zeolite as a hybrid basic catalyst. Catal Lett. 2016;146:2200-2213.
14. Sing K.S.W. Reporting physisorption data for gas/solid systems with special reference to the determination of surface area and porosity (Provisional). Pure Appl Chem. 1982;54:2201-2218.
15. Jabariyan Sh., Zanjanchi M.A. A simple and fast sonication procedure to remove surfactant templates from mesoporous MCM-41. Ultrason. Sonochem. 2012;19:1087-1093.
16. Shekofteh-Gohari M., Habibi-Yangjeh A. Fabrication of novel magnetically separable visible-light-driven photocatalysts through photosensitization of Fe_3O_4/ZnO with $CuWO_4$. J Indus Eng Chem. 2016;44:174-184.
17. Yang Y., Zhang G., Xu W. Facile synthesis and photocatalytic properties of Ag/AgCl/TiO_2/rectorite composite. J Colloid Interface Sci. 2012;376:217–223.
18. Wang C.C., Lee C.K., Lyu M.D., Juang L.C. Photocatalytic degradation of C.I. Basic Violet 10 using TiO_2 catalysts supported by Y zeolite: an investigation of the effects of operational parameters. Dyes Pigments. 2008;76:817–824.
19. Macedo L.C., Zaia D.A.M., Moore G.J., Santana H. Degradation of leather dye on TiO_2: a study of applied experimental parameters on photoelectrocatalysis. J. Photochem Photobio A. 2007;185:86–93.
20. Xu Y., Schoonen M.A.A. The absolute energy positions of conduction and valence bands of selected semiconducting minerals. Am Mineral. 2000,85:543–556.
21. Zhang X., Chen Y.L., Liu R.S., Tsai D.P. Plasmonic photocatalysis. Reports on Progress in Physics. Rep Prog Phys. 2013;76:046401-046442.
22. Zhang L.S., Wong K.H., Yip H.Y., Hu C., Yu J.C., Chan C.Y., Wong P.K. Effective photocatalytic disinfection of E. coli K-12 using AgBr-Ag-Bi_2WO_6 nanojunction system irradiated by visible light: the role of diffusing hydroxyl radicals. Environ Sci Technol. 2010;44:1392–1398.
23. Li G.T., Wong K.H., Zhang X.W., Hu C., Yu J.C., Chan R.C.Y., Wong P.K. Degradation of ccid orange 7 using magnetic AgBr under visible light: the roles of oxidizing Species. Chemosphere. 2009;76:1185–1191.
24. Zhang N., Liu S.Q., Fu X.Z., Xu Y.J. Synthesis of M@TiO_2 (M = Au, Pd, Pt) Core–shell nanocomposites with tunable photoreactivity. J Phys Chem C. 2011,115:9136–9145.
25. Tong H., Ouyang S., Bi Y., Umezawa N., Oshikiri M., Ye J. Nano-photocatalytic materials: possibilities and challenges. Adv Mater. 2012;24:229–251.
26. Liu H.R., Shao G.X., Zhao J.F., Zhang Z.X., Zhang Y., Liang J., et al. Worm-like Ag/ZnO core-shell heterostructural composites: fabrication characterization, and Photocatalysis. J Phys Chem C. 2012;116:16182–16190.
27. Jadhav J., Biswas S. Surface plasmon enhanced near-UV emission in monodispersed ZnO: Ag core-shell type nanoparticles synthesized by a wet chemical method. Superlattices Microstruct. 2016;91:8–21.
28. Liu Y., Wei Sh., Gao W. Ag/ZnO heterostructures and their photocatalytic activity under visible light: Effect of reducing medium. J Hazard Mater. 2015;287:59–68.